buildings

MDPI

Article

Performance Comparison of Different Building Shapes Using a Wind Tunnel and a Computational Model

Dany Perwita Sari [1,*] and Kang-Pyo Cho [2]

[1] Research Center for Biomaterials, National Agency for Research and Innovation (BRIN), Cibinong 16911, Indonesia
[2] CKP Wind Solutions, Gimje-si 992-73, Korea; kpcho@ckpwind.com
* Correspondence: dany.perwitasari@gmail.com; Tel.: +62-851-56851970

Abstract: A building-integrated wind turbine (BIWT) is an alternative way to assess renewable energy. BIWTs produces their own energy without relying on fossil fuels. However, only a few researchers have studied BIWTs. Greater wind velocity (V) results in greater potential energy (P). The aerodynamic design has an important role to play in increasing wind velocity and reducing turbulence intensity. CFD simulations taken from previous research have revealed that round-shaped buildings increase velocity up to 30%. This study focuses on the wind response of square and top-rounded-shaped building models, and their optimization based on variations in wind velocity. Wind tunnel studies were conducted to study wind flow around the building, followed by a computer simulation to verify the results. In a wind tunnel, three BIWT models (1:150 in scale) located in Seoul, South Korea (terrain B), were evaluated. The results of the study show that the streamline should be followed when installing wind turbines on rectangular rooves with flat surfaces. This method allows wind speed to be elevated significantly, when compared to a turbine at a higher height. In addition, round corners can produce wind velocity that is up to 34% greater than sharp corners beside a building. In summary, this paper presents a five-step analysis framework that can be used by researchers who wish to analyze BIWTs through wind tunnel experiments and CFD.

Keywords: urban wind energy; high-rise building; round-shape building; building-integrated wind turbines; CFD simulation; wind tunnel

Citation: Sari, D.P.; Cho, K.-P. Performance Comparison of Different Building Shapes Using a Wind Tunnel and a Computational Model. *Buildings* **2022**, *12*, 144. https://doi.org/10.3390/buildings12020144

Academic Editors: Nikos A. Salingaros, Alexandros A. Lavdas, Michael W. Mehaffy and Ann Sussman

Received: 30 December 2021
Accepted: 25 January 2022
Published: 29 January 2022

1. Introduction

The global population is growing rapidly, which increases energy demand proportionally [1]. Global warming is a phenomenon related to temperature increases on the surface of the planet [2]. As a result of global warming and energy crisis issues, alternative energy has become one of the most mature renewable energies in urban areas. As one of the largest renewable energy sources, wind energy has currently gained the most traction [3–6]. Moreover, the current trend indicates that wind energy will continue to be the leading renewable power source for the foreseeable future, continuing to garner the highest investments and having the highest number of new installations [6].

There is a strong correlation between global warming and building energy performance [7–9]. Most of the world's buildings represent large energy consumers, contributing significantly to global warming. In urban areas, most high-rise buildings have been estranged from nature and completely separated from it. Recent years have seen a significant increase in wind generation in urban settings known as building-integrated wind turbines (BIWTs). As wind changes speed with height (boundary layer), generating energy on rooftops is of great importance to reduce the generation load and transmission losses [10,11], since one of the most important characteristics of wind is its variation with height. BIWTs are installed wind turbines that are completely integrated into the architectural design of buildings, for instance, within/on the corners of the façades or between the buildings

(Figure 1) [12]. BIWT is becoming more common as a new green building icon and a new way to assess optimal energy use in buildings [10,13]. It has several benefits, such as decentralized power generation, reduced transmission losses and reduced construction costs.

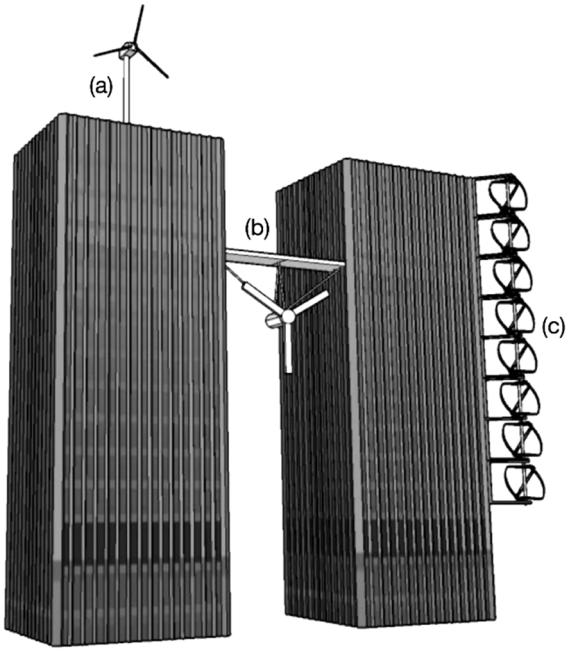

Figure 1. BIWT model and the possible location of wind turbines (**a**) on top of a building, (**b**) between two buildings, and (**c**) in the side of a building.

A designer should analyze carefully when designing BIWTs, especially regarding urban areas and local weather conditions [14]. The building has to be shaped in a way that maximizes wind harvesting in the chosen urban environment. Due to complex building arrangements, wind speed in urban areas tends to be affected by surface roughness. The main parameters that affect the efficiency of wind turbines on tall buildings in urban environments are the building's geometry, and inflow wind characteristics [15]. These geometries, especially different roof shapes, determine the amounts of power density and turbulence intensity around high-rise buildings in urban areas [14,16]. The large turbulence intensity and the small wind velocity of the incoming flow impinging on buildings reduce the efficiency of wind turbines [17]. However, in previous studies, analysis based on the computation of fluid dynamics (CFD) simulations showed that rounded-shape buildings can increase velocity by as much as 30% [18]. Rounded-corner models had the most efficient performance in reducing drag coefficient, as compared to the others [19]. To employ BIWTs, it is important to design the building shape and swept area carefully to increase wind velocity.

In light of the lack of research on the BIWT, either experimentally or academically, we conducted this study. In this study, three different BIWTs were modeled by aerodynamically modifying the rooftop with rounded corners and $\frac{1}{2}$ rounded, compared with a basic, rectangular flat roof. All models were analyzed primarily using wind tunnel experiments. Many wind tunnel studies conducted in the 20th century have produced highly accurate quantitative analyses [20–22]. Wind tunnel experiments are conducted in order to predict the effects of wind on buildings. In the design of high-rise structures, wind effects are generally a major concern, especially when wind turbines are included. A Cobra probe and a pitot tube were used to measure the results. As a comparison, a computational model was selected for validating the data. Rather than directly comparing the CFD/wind tunnel experiments, this research emphasizes the conclusions that can be drawn from the results. The purpose of this experiment was to explore potential wind energy in urban areas using models, in order to find the most efficient BIWT design.

1.1. Research Questions

1. If the wind turbine is installed on top of a building, what is the recommended roof shape?
2. How does the location of the wind turbines and the intensity of the turbulence affect each other?
3. What are the best ways to measure wind velocity, turbulence intensity, and wind potential in a wind tunnel?
4. What are the results of the wind tunnel experiment in comparison with the CFD simulation? This research will focus on achieving the following objectives.

1.2. Research Objectives

1. To compare the best aerodynamic shapes to increase wind velocity, using different building shapes.
2. To identify whether wind flow can be measured around a building using cobra probes.
3. To identify whether pitot tubes can be used as a comparison tool with cobra probes in the same wind tunnel experiment.
4. To compare the velocity coefficient and turbulence intensity of the measured data using multiple points.

2. Material and Methods

2.1. Evaluating the Performance of Wind Turbines

The design of a BIWT depends on the accurate prediction of output power. The high-rise building's placement of wind turbines is meant to catch high-velocity winds on a high altitude [18]. A wind turbine's power can be calculated using its potential energy (P). Potential energy from the wind can be calculated using this equation:

$$P = 1/2\ \rho\ A\ C_p\ V^3 \quad (1)$$

where P is wind turbine power, C_p is the coefficient of performance, ρ is air density, A is the swept area of the blades, and V is wind velocity. The power of the turbine is highly dependent on the speed of the wind (V). When the wind speed doubles, the power increases by eight times. In addition to the height of the building, the shape of the building can also increase wind velocity. Building architecture can be designed to capture and tunnel wind through the turbines, which can produce wind speeds greater than the prevailing wind speed. Aerodynamics models are based on this design. As the shapes and spatial relationships of the tower sculpt the airflow, the wind velocity increases.

2.2. Physical Model

From Equation (1), it is crucial to properly design a BIWT's aerodynamic shape and swept area (A) to increase wind speed (V). Based on this basic concept, three aerodynamic shapes were developed. This study analyzes three aerodynamic performances, each with its own roof pattern. Figure 2 shows the atmospheric boundary layer wind tunnel of the CKP wind tunnel [23] where the experiments were conducted, and the basic models used in the present study. The experimental data was collected using the cobra probe, an instrument calibrated regularly in the CKP wind tunnel. The wind tunnel experiments are conducted on a building model (scale 1:150) with dimensions of 16 m × 16 m × 64 m. The models were analyzed in Seoul, South Korea, as a representative location. The BIWT was located in terrain B [24,25] which describes urban areas with numerous closely spaced obstructions having the size of single-family dwellings with the height of 3.5 m. A power law (2) can be used to approximate the wind speed profiles within atmospheric boundary layers, which belong to the turbulent boundary layer type. Wind speed profile can be seen in Figure 3, where Z is height and U is average wind speed in Z.

$$V_{(z)} = V_1\ (Z/Z_1)^{\alpha} \quad (2)$$

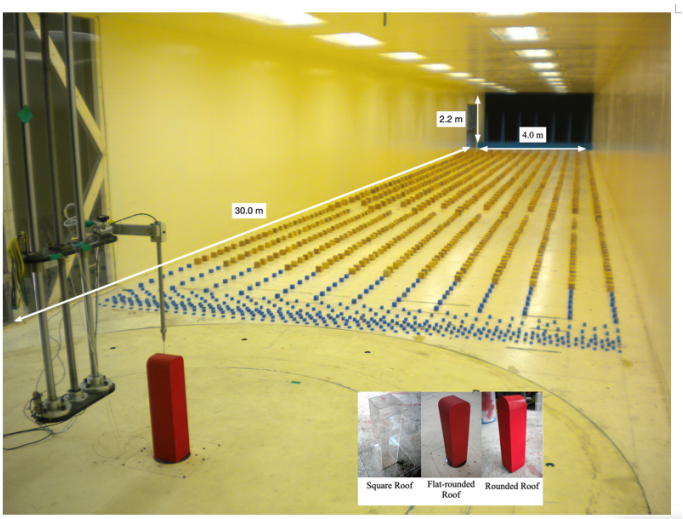

Figure 2. Building shape models (square roof, rounded corner roof, rounded roof) in CKP wind solution's atmospheric boundary layer wind tunnel.

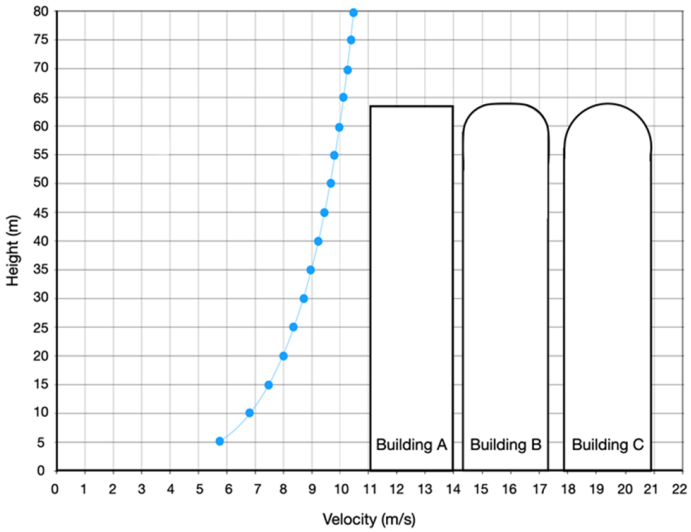

Figure 3. The wind velocity profile from the Power Law Equation (2) in terrain B at the height of the building (scale 1:150).

The building model was composed of 2 mm thick acrylic sheets attached with glue. Experimental measurements were completed on the top of the building at specific points during wind tunnel tests. Figure 4 shows that a wind turbine is situated on the roof of a building. Various locations on the model were used to measure each building. Wind tunnel experiments were conducted for three different building types. First building (Figure 4a) was a common rectangular shape, later called building A. The turbine was located in front, along the wind, because the highest wind velocity is the windward surface of the building. The higher the tower of the wind turbine is, the larger the wind velocity is [18,26]. Because of that reason, in this experiment we used a height 35 mm (5 m) above the roof of the building A. The second building (Figure 4b) was a rectangular shape with rounded-corner shape on the top of the building, later called building B. For the last model, we modified the roof shape with a $\frac{1}{2}$ circular. The turbine was located in the middle of the building (Figure 4c), and later called building C.

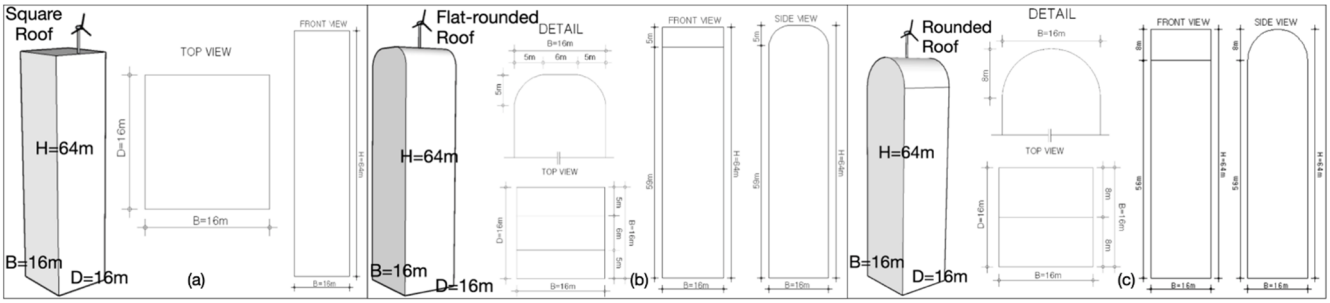

Figure 4. Detailed geometry of the building models (scale 1:150) used for the experiments: (**a**) square roof building A, (**b**) rounded-corner roof building B, and (**c**) round roof building C.

2.3. Measure Tools

Cobra probes were used in the wind tunnels to calculate wind velocities and turbulence intensity (Figure 5a). The cobra probe or dynamic multi-hole pressure probe measured the mean and fluctuating 3-component velocities (Figure 5a), as well as the static pressure [27]. Building A was measured by cobra probes only. This is because the design of the building was not complicated. In the case of building B, pitot tubes were used as a comparison for cobra probes due to the rounded shape. The same method was used for building C, which was a cobra probe and pitot tube calibration (Figure 5c). Pitot tubes are the basic instrument for measuring wind speed in wind tunnels. By using the pitot tube, the local velocity can be determined at any given point in the flow stream, as opposed to the average velocity of the pipe or conduit. Figure 5b shows the basic pitot tube, which consists of a tube pointing directly into the fluid. The pressure in this tube can be measured since fluid exists within it. However, the flow of fluid is brought to a halt (stagnates), since there is no outlet to allow flow to continue. The pitot tube operates on the principle of converting kinetic energy into pressure at a stagnation point. This instrument is accurate, reliable, convenient, and economical. To convert stagnation pressure to fluid velocity, use Bresnoulli's Equation (3):

$$\text{Total pressure} = \text{static pressure} + \text{dynamic pressure} \tag{3}$$

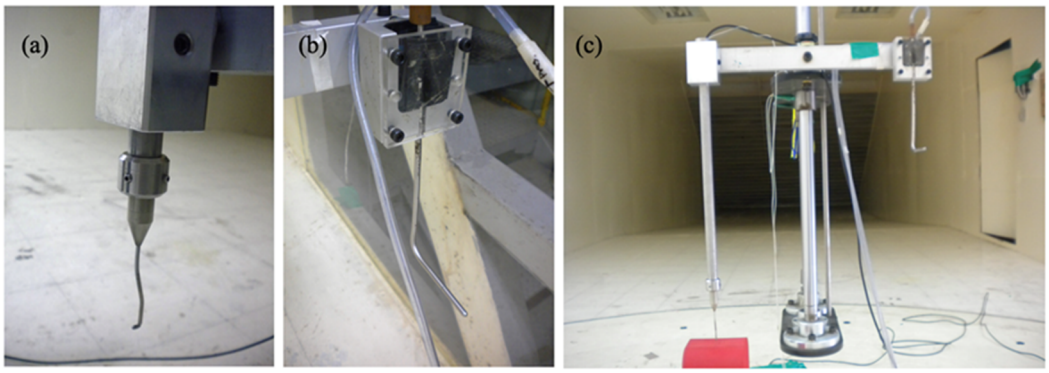

Figure 5. The measurement tools for building models in a wind tunnel are (**a**) cobra probes, (**b**) pitot tubes. (**c**) A demonstration on how to arrange the tools in a wind tunnel.

To calculate the velocity (4):

$$V^2 = \frac{2(Pt - Ps)}{\rho} \tag{4}$$

However, the pitot tube is inaccurate at low speed (about less than 5 m/s) and unsuitable for measuring turbulence. This weakness can be measured using cobra probes, which

can measure low wind speeds. Moreover, there were differences in the wind tunnel experiment results between the cobra probes and the pitot tube. Because of this, the researcher made a simple experiment with a new equation, as shown in Table 1. The result from Table 1 can be drawn upon to become linear regression (Figure 6). The relation between the pitot tube and the cobra probe can be describe by:

$$y = 1.055x + 0.124. \quad (5)$$

Table 1. Simple experiment to equate the wind tunnel result between the pitot tube and the cobra probe.

Sampling time (s): 20.480 Number of samples: 12,800 Data output rate (Hz): 625.0				
Calibration	**Experiment (m/s)**			
	1	**2**	**3**	**4**
Pitot tube$_1$		2		
Cobra probe$_1$	2.25	2.27	2.23	2.14
Pitot tube$_2$		4.1		
Cobra probe$_2$	4.31	4.24	4.26	4.36
Pitot tube$_3$		6.13		
Cobra probe$_3$	6.49	6.35	6.57	6.6
Pitot tube$_4$		8.22		
Cobra probe$_4$	8.7	8.74	8.62	8.74
Pitot tube$_5$		10.1		
Cobra probe$_5$	10.6	10.5	10.5	10.7

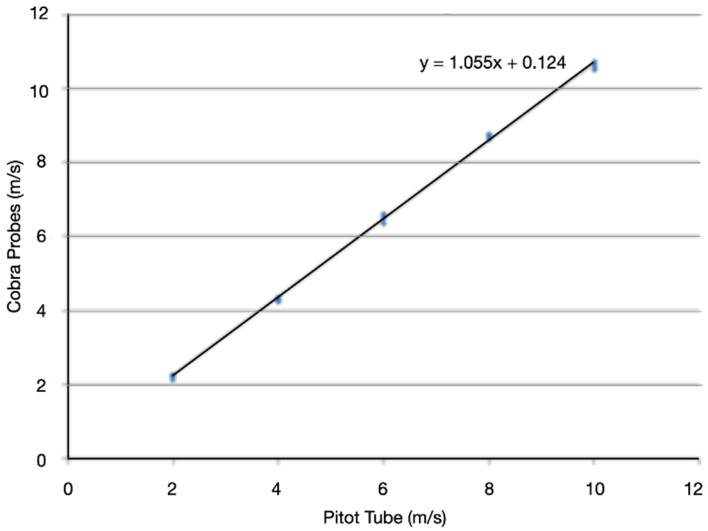

Figure 6. Linear regression wind velocity result between pitot tube and cobra probes.

The equation result (5) can identify the similarities between the pitot tube and the cobra probe's wind velocity results (Figure 6).

3. Experimental Results and Discussion

The wind tunnel experiment is widely accepted by scientific and engineering communities. This method has proven to be accurate and representative of real-world situations when it correctly accounts for the characteristics of the atmosphere, and when the model is scaled correctly, as is already widely accepted worldwide for the analysis of wind turbines

or building structures. Turbulence intensity can also be calculated during experiments using wind tunnels. All models in wind tunnel tests must be conducted under similarity parameters, such as:

1. Geometric similarity: the model must be the same shape as the prototype, including the structure to be tested, its surroundings, boundary layer thickness, and turbulence length scale.
2. Kinetic similarity: to achieve kinematic similarity, it is essential to analyze turbulence intensity, duration, and distribution of turbulence scales, roughness block, and the boundary layer, as well as power spectral density.
3. Mechanical similarity: similarities in mechanical motion can also be defined by Reynolds numbers, natural periods, mass ratios, elastic parameters, and damping constants.
4. In building A, cobra probes were used to measure wind velocity at the curtain point. Cobra probes and pitot tubes were used in building B and building C.

In this experiment, the results are shown as velocity coefficients (VC) (6) derived from the velocity at point (x), divided by the boundary layer velocity in terrain B.

$$\text{Velocity Coefficient (VC)} = V_{\text{in point}}/V_{\text{approach}} \quad (6)$$

Each model contained wind turbines located on top of the building, and between 50 m (buildings B and C) and 70 m (building A) above ground (Figure 7). The average wind velocity ($V_{approach}$) was 10m/s.

3.1. Building A

For building A, wind turbines were located in the windward side of the building, since most of the wind velocity is experienced there (Figure 7a). The wind turbine was estimated to be five meters tall. Wind turbines were set up in this experiment at a height of 5 m above the roof. The further back the wind was, the higher the wind speed; the further back the wind location, the higher the velocity was (Figure 8). The best positions for wind turbines were at 8, 10, and 12, with VC values of 11.8. On those points, especially starting from points 10 to 12, the intensity of the turbulence increased as well. However, it was still lower than TI inlet, except for point 11.

Cobra probes provided important turbulence intensity data for structural engineers. The blade flicker can be prevented by controlling the turbulence intensity. In this case, wind turbines were recommended for installation in points 4 through 10. As the vortex has not yet been created in front of the building. Additionally, the location of the wind turbine in point 11 is not recommended. Overall, wind velocity grew by 10% from the wind velocity approach (Figure 8), with more stable TI in front, and fluctuating TI at the back.

3.2. Building B

The wind turbines in Building B were located in the middle roof after passing through a rounded corner (Figure 7b). The elevation of the wind turbines varied from 1m to 10m above the roofline. We used a method for measuring B by using cobra probes and pitot tubes; a pitot tube was used to validate the results of the cobra probe. In Figure 9, the wind flow increased instantly after passing the rounded corner (VC on point 1 = 1.24), but then decreased as the point got higher (VC on point 30 = 1.16). After passing through the rounded shape at a height of 1 to 4 m above the roof surface, the wind velocity increased. Above a height of five to ten meters, wind speeds tended to stabilize. Even so, this value was higher than the wind velocity inlet (VC inlet = 1). Compared to building A, these results were completely different.

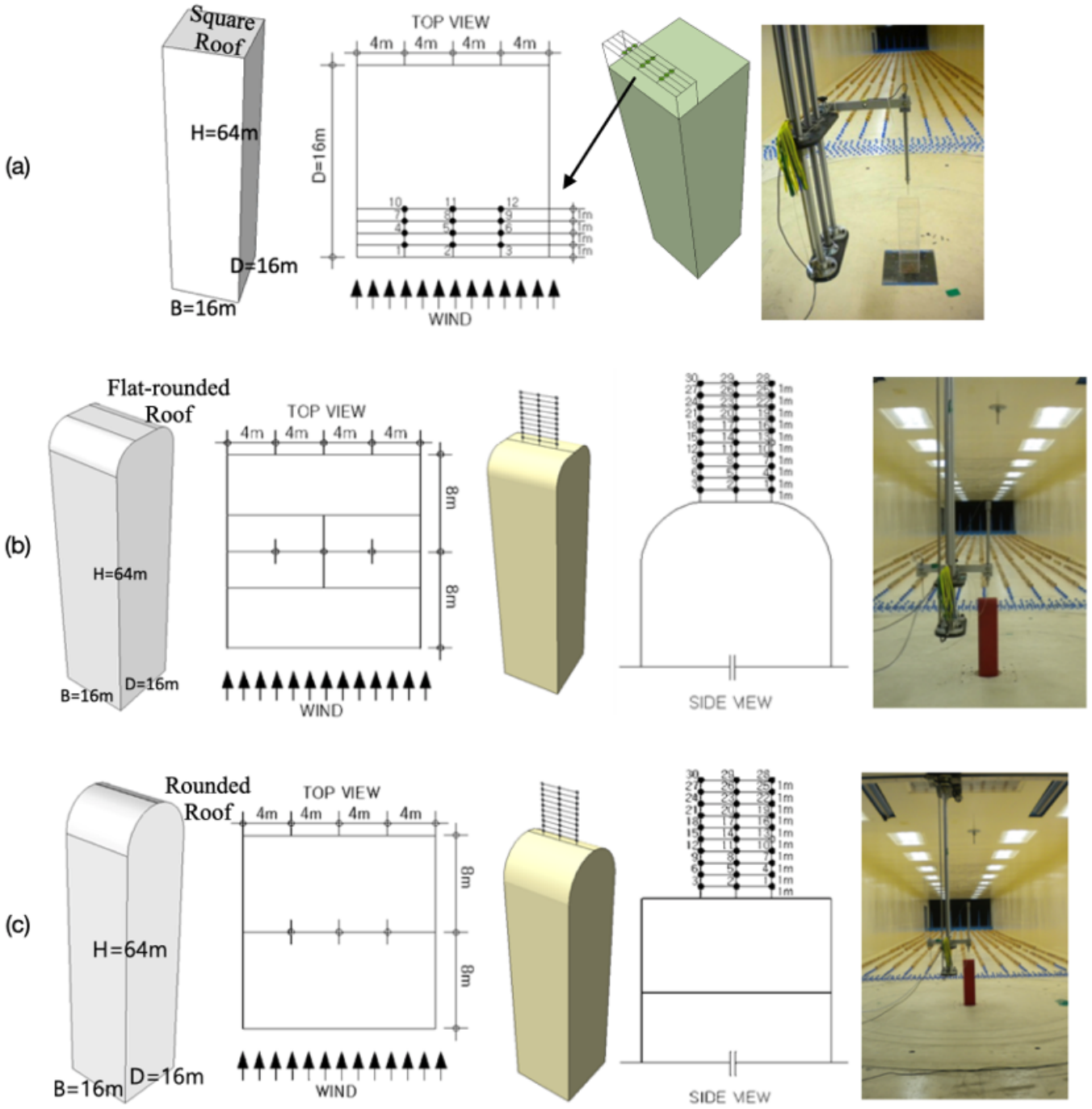

Figure 7. Wind turbine position at: (**a**) windward surface 5 on the top of the building; (**b**) windward surface 1 m up to 10 m on the top of the building; (**c**) windward surface 1 m up to 10 m on the top of building.

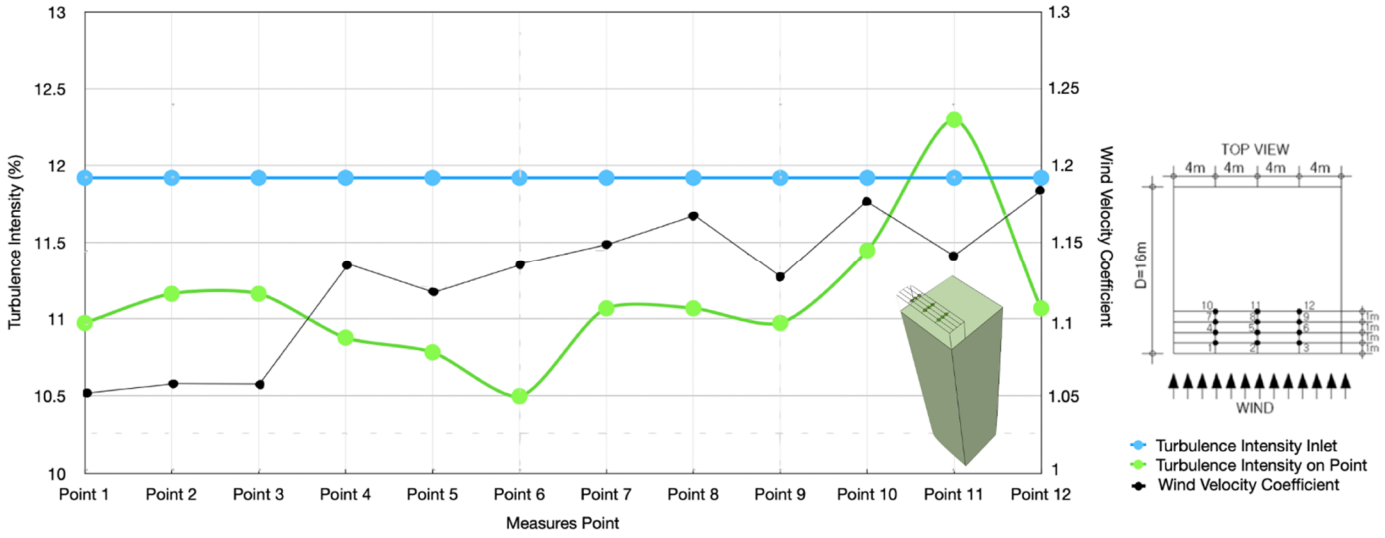

Figure 8. A wind tunnel test on Building A resulted in a measurement of the velocity coefficient (VC) and turbulent intensity (TI). Wind turbines were recommended to be installed in points 4 through 10, with an overall increased wind velocity of 10% over the wind velocity approach. With the exception of point 11, TI percentages were lower than the TI inlet.

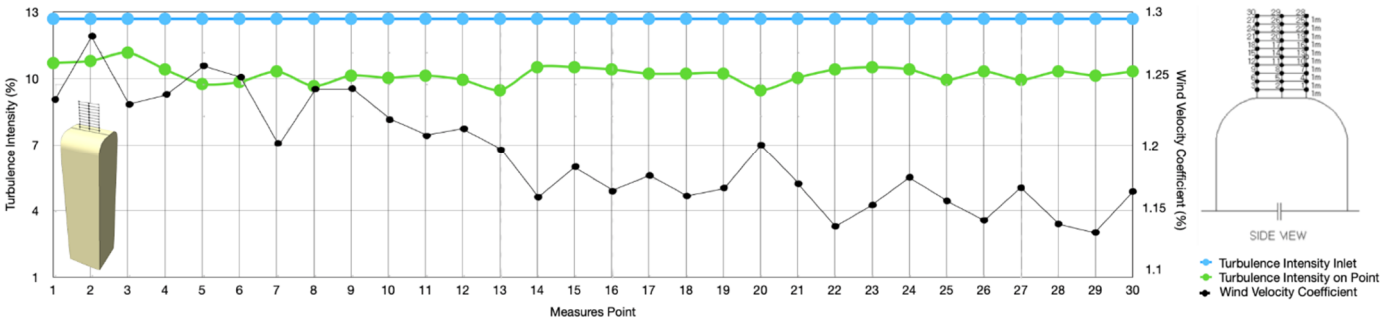

Figure 9. A wind tunnel test on building B resulted in a measurement of the velocity coefficient (VC) and turbulent intensity (TI). Wind velocity increased by 29% with rounded corners. In this design, a wind turbine was best placed at points 1 to 9 (1 m to 3 m above the roof).

The TI results for building B (Figure 9) were relatively stable, between (9% to 12%). Additionally, the $TI_{on\ point}$ was lower than the TI_{inlet} (12.9% respectively). Higher wind velocity in lower areas with stable TI was mainly because round-cornered buildings increase laminar flow, rather than turbulent flow. As a result of these rounded corners, wind velocity increased by 29%. In this design, a wind turbine was best placed at points 1 to 9 (1 m to 3 m above the roof). As a result of this shape modification, designers do not need to install tall wind turbine towers, such as in building A (5 m above the roof).

3.3. Building C

For building C's roof, $\frac{1}{2}$ circular shapes were planned. The wind turbines were in the center of a rounded shape at a height of 1 m up to 10 m (Figure 7c). Similar to building B, building C measurements were taken with cobra probes and pitot tubes. The VC trends in each point were almost the same as in building B, although they were more stable, and higher (Figure 10). The highest point was at point 1 (VC = 1.34), and the lowest was at point 30 (VC = 1.25). From point 1 to 30 (11% respectively), TI were stable, and lower than the TI inlet (12.5% respectively). Adding the circular shapes increased laminar flow and reduced wind pressure.

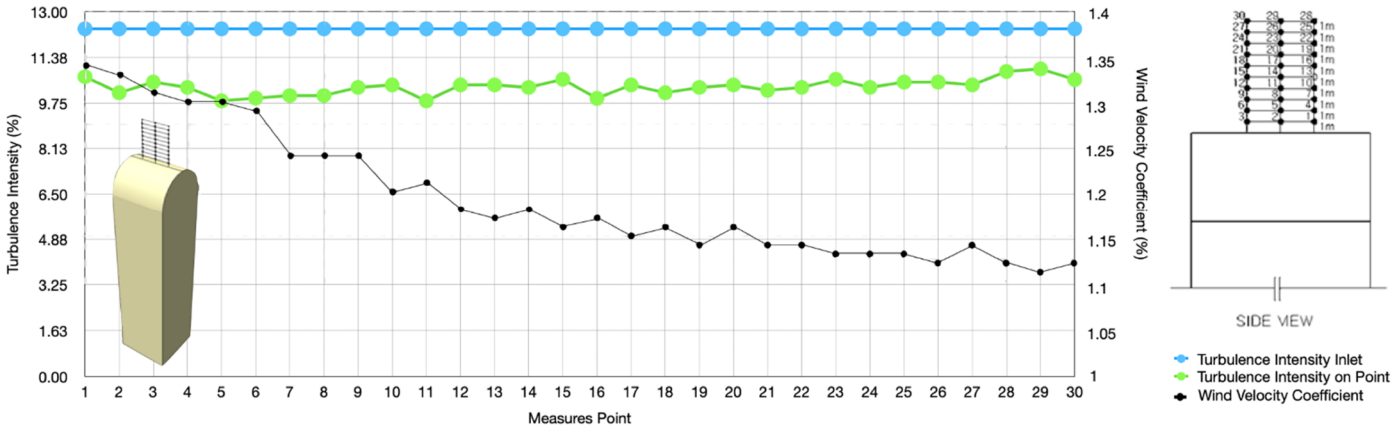

Figure 10. A wind tunnel test on building C resulted in a measurement of the velocity coefficient (VC) and turbulent intensity (TI). The $\frac{1}{2}$ round shape can produce wind velocity up to 34% greater than other shapes. In this model, wind turbines should be installed in the 1 m to 2 m height above the $\frac{1}{2}$ rounded shapes.

The $\frac{1}{2}$ round shape can produce wind velocity up to 34% greater than other shapes. When compared with other models, building C had the best performance. In this model, wind turbines should be installed in the 1 m to 2 m height above the $\frac{1}{2}$ rounded shape. Keeping the wind turbine tower lower can increase wind velocity with a fully rounded shape.

4. Comparison of Wind Tunnel Results with Computer Simulation

A comparison with CFD analysis from previous results was also performed to obtain a better understanding of wind flow [18,28]. A combination of these methods was used to validate the model's results. In comparison to a regular experiment, the CFD provides much more detailed information about the flow field. To study wind flow around a building, CFD is a powerful analysis tool. In addition, it is inexpensive, and the results can be repeated numerous times. A CFD model can be used to determine optimal positions and wind speeds for turbines under different wind conditions [18,29]. The simulation of wind flows on the roof of the building will help us understand the flow. Simulation settings were similar to those used in a wind tunnel experiment, including the building shape, building scale (1:150), building location, terrain, and velocity input (10 m/s). Models were set in the boundary layer of terrain B with viscous K-epsilon, and all of the iterations were successful.

As compared to building B and building C, building A could not increase wind velocity optimally. Computer simulations and experiments have shown that the higher the tower of a wind turbine is, the larger the wind velocity (Figure 11a). An experiment in the wind tunnel indicated that wind velocity was stable at VC = 1.2. This trend was also reflected in the computational simulation, where VC = 1.1 (Figure 12a). Overall, the results of the experiment were nearly identical to those of the simulation (Figure 11b).

In building B, the wind turbines were located in the center of the roof. After passing through the round corner (Figure 11b), the wind velocity increased. Figure 12b shows similar results for CFD and the wind tunnel. Point 2 had the highest VC in both the wind tunnel experiments (VC = 1.29) and the computational simulation (VC = 1.24). After passing through the rounded shape (Figure 11b), the wind velocity increased. The results of the wind tunnel and CFD were almost identical (Figure 12b). Approach wind velocity increased by roughly 25–29%.

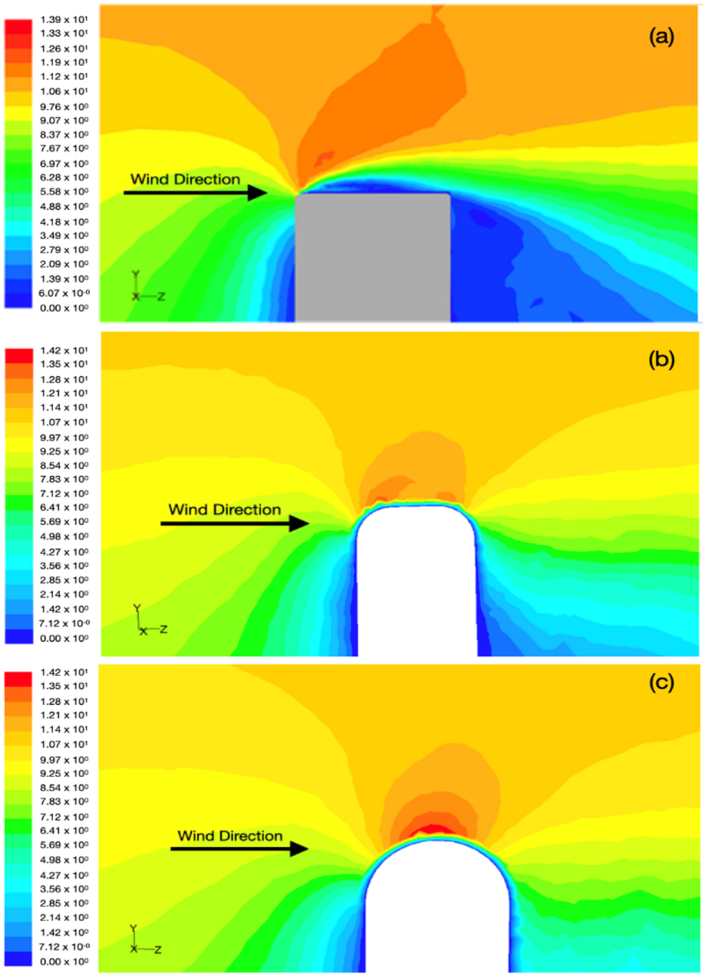

Figure 11. Contour plots of wind velocity magnitude on the side view (X-coordinate) (**a**) building A shows the highest velocity located windward the building; (**b**) building B shows the highest velocity near the rounded shape in front and back the building; (**c**) building C shows the wind velocity is more stable, centered in the middle.

Building C experienced an increase in wind speed after passing the rounded shape in the middle of the rounded shape (Figure 11c). Red color contour in Figure 11c indicated the increase in wind speed. The wind speed dominates the middle of the $\frac{1}{2}$ rounded shape in heights of 1–2 m. A similar result was found using both wind tunnels and CFD (Figure 11c). The wind tunnel experiment showed that point 1 had the highest VC (1.34). However, for CFD, the highest VC was found in point 2 (VC = 1.35). Wind velocity increased by 35% from the wind velocity approach (Figure 12c).

A comparison of three BIWT models was conducted (building A, building B, and building C). Overall, all three models were in good agreement with the experimental data, but building C provided the best performance. Furthermore, the computed simulations supported these findings. These studies were conducted with a building model of a single building and not interrupted by urban morphology, such as another building or three. The model assumed that any local impacts of the surrounding objects on the wind speed were excluded, such as the mutual influence of the turbines on one another's performance and the local flow signature of the building.

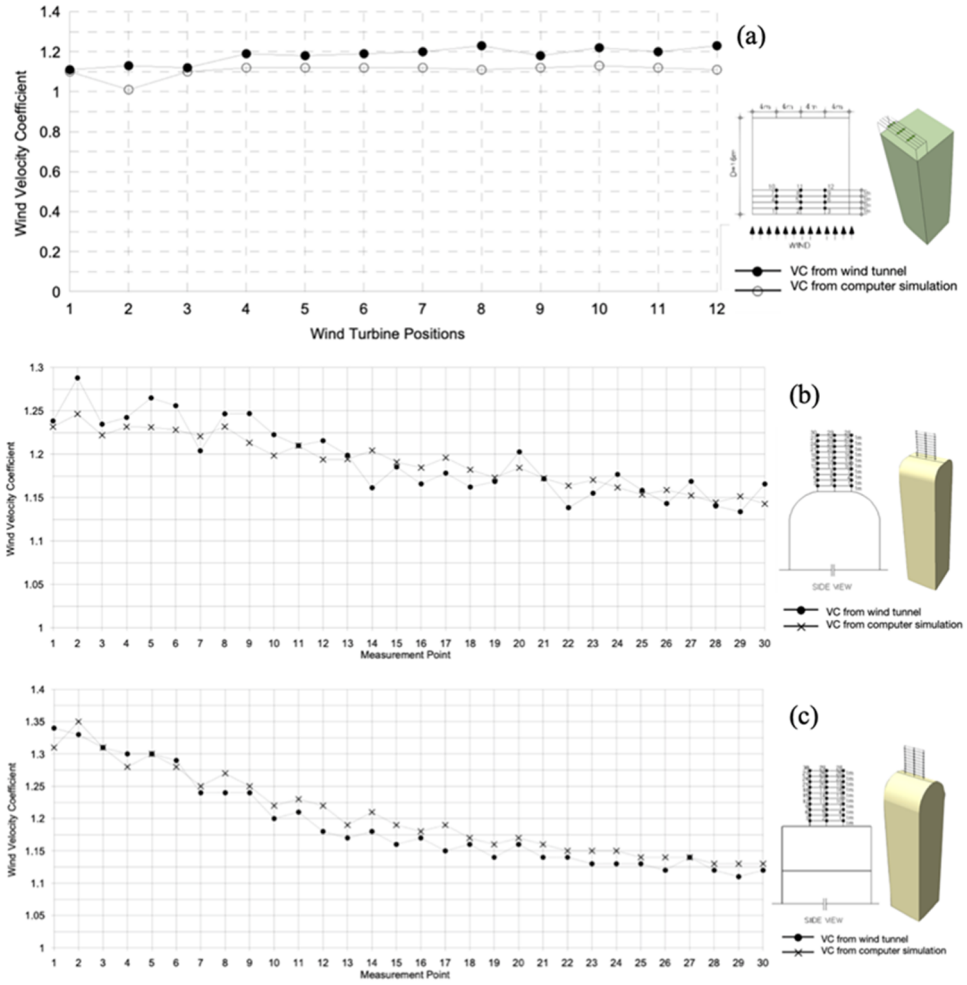

Figure 12. Velocity coefficient (VC) results from wind tunnel experiment and computer simulation on (**a**) building A, (**b**) building B, (**c**) building C. Overall the wind flow patterns were similar and the VC were similar.

5. Conclusions

An aerodynamic investigation on wind flow and wind velocity of BIWTs using wind tunnel experiments and computer analysis has been briefly introduced in this study. Putting wind turbines on top of buildings (BIWTs) should allow them to take advantage of building height without having to construct expensive, full-size towers, especially in urban areas. The framework this study was based on consisted of the following simple steps:

- *Step 1*: Designing the building. Using references from various aerodynamic shapes that apply to BIWTs.
- *Step 2*: Setting up the wind tunnel experiment: geometric similarity, kinetic similarity, mechanical similarity, and tool calibration.
- *Step 3*: Conducting a wind tunnel experiment. Research in wind tunnels using two measurement tools (cobra probes and pitot tubes) in order to make the prediction more accurate, especially in rounded shapes. The cobra probes measured turbulence intensity and wind velocity. The pitot tube was used for comparison.
- *Step 4*: Performing a computational analysis. Evaluating multiple BIWT models using computer models and creating model variables similar to those in the wind tunnel. Using a similar scale to that used in the experiment, and simplifying the models to reduce errors.
- *Step 5*: Validating the CFD and wind tunnel experiment results.

For a simple rectangular building with flat roof shapes, it is important to locate wind turbines following the streamline. This method can increase wind velocity effectively when compared with built higher turbines. When modifying the building top, a the rounded-corner shape could increase wind speed (25–29% from approach wind velocity) if compared with a flat, sharp, corner top. For the 1/2 rounded-shape on the roof (without a flat area), the streamline looked steadier at the center. The wind speed increased at the center of the rounded towers (35% from approach wind velocity).

The wind turbine should be installed to the windward side of each of these designs. In order to install a wind turbine with 5 m height inside a simple rectangular building with a flat roof, the turbine needs to be situated 4 m to the front of the building. The wind velocity method can increase the wind velocity by up to 10%. Installing rounded corners on rooves has the potential to increase wind speed by as much as 29%, by only installing the wind turbines 3 m above the ground and positioning them in the middle of the roof building. A half-round roof building has the best performance. Increased wind velocity (up to 34%) is possible with a lower wind turbine tower (1 m to 2 m at the middle of the roof). Circular shapes increase laminar flow, decrease wind pressure, and stabilize turbulence intensity.

Performing experiments is challenging and requires time. This includes evaluating different sources of error. In this case, the errors were due to the instruments and measurement methods. On one hand, CFD errors were a result of the messing techniques and parameter classification. In general, both methods were accurate. According to this study, wind tunnel experiments and computer simulation show similar results and patterns. In order for these similarities to occur, detailed simulation settings variables are needed.

Author Contributions: Conceptualization, D.P.S.; methodology, D.P.S. and K.-P.C.; software, D.P.S. and K.-P.C.; validation, D.P.S. and K.-P.C.; formal analysis, D.P.S.; investigation, D.P.S.; resources, K.-P.C.; data curation, D.P.S.; writing—original draft preparation, D.P.S.; writing—review and editing, D.P.S.; visualization, D.P.S.; supervision, D.P.S. and K.-P.C.; project administration, K.-P.C.; funding acquisition, K.-P.C. All authors have read and agreed to the published version of the manuscript.

Funding: This research received no external funding.

Institutional Review Board Statement: Not applicable.

Informed Consent Statement: Not applicable.

Acknowledgments: The author of this study carried out this research under the support of CKP Wind Solutions.

Conflicts of Interest: The authors declare no conflict of interest.

References

1. U.S. Energy Information Administration (EIA): International Energy Outlook 2016. Available online: www.eia.gov/forecasts/ieo (accessed on 2 November 2021).
2. U.S. National Aeronautics and Space Administration (NASA): Global Temperature. Available online: https://climate.nasa.gov/vital-signs/global-temperature/ (accessed on 2 November 2021).
3. European Renewable Energy Council (EREC): Rethinking 2050: A 100% Renewable Energy Vision for the European Union. Available online: www.erec.org (accessed on 2 November 2021).
4. Global Wind Energy Council (GWEC): Global Wind Statistics 2021. Available online: https://gwec.net/global-wind-report-2021/ (accessed on 2 November 2021).
5. World Wind Energy Association: REN21's Renewables 2018—Global Status Report (GSR). Available online: https://www.ren21.net/reports/ (accessed on 3 January 2019).
6. European Environment Agency, Renewable Energy in Europe 2017: Recent Growth and Knock-On Effects (EEA Report No. 3/2017). Available online: https://www.eea.europa.eu/publications/renewable-energy-in-europe-2017 (accessed on 4 March 2020).
7. Campagna, L.M.; Fiori, F. On the Impact of Climate Change on Building Energy Consumptions: A Meta-Analysis. *Energies* **2022**, *15*, 354. [CrossRef]
8. Rodríguez, M.V.; Cordero, A.S.; Melgar, S.G.; Márquez, J.M.A. Impact of Global Warming in Subtropical Climate Buildings: Future Trends and Mitigation Strategies. *Energies* **2020**, *13*, 6188. [CrossRef]

9. Dodoo, A.; Ayarkwa, J. Effects of Climate Change for Thermal Comfort and Energy Performance of Residential Buildings in a Sub-Saharan African Climate. *Buildings* **2019**, *9*, 215. [CrossRef]
10. Ishugah, T.F.; Li, Y.; Wang, R.Z.; Kiplagat, J.K. Advances in wind energy resource exploitation in urban environment: A review. *Renew. Sust. Energ. Rev.* **2014**, *37*, 613–626. [CrossRef]
11. Walker, S.L. Building mounted wind turbines and their suitability for the urban scale: A review of methods of estimating urban wind resource. *Energy Build.* **2011**, *43*, 1852–1862. [CrossRef]
12. Rezaeihaa, A.; Montazeri, H.; Blocken, B. A framework for preliminary large-scale urban wind energy potential assessment: Roof-mounted wind turbines. *Energy Convers. Manag.* **2020**, *214*, 112770. [CrossRef]
13. Grant, A.; Johnstone, C.; Kelly, N. Urban wind energy conversion: The potential of ducted turbines. *Renew. Energy* **2008**, *33*, 1157–1163. [CrossRef]
14. Juan, Y.H.; Wen, C.Y.; Li, Z.; Yang, A.S. Impacts of urban morphology on improving urban wind energy potential for generic high-rise building arrays. *Appl. Energy* **2021**, *299*, 117304. [CrossRef]
15. Skvorc, P.; Kozmar, H. Wind energy harnessing on tall buildings in urban environments. *Renew. Sust. Energ. Rev.* **2021**, *152*, 111662. [CrossRef]
16. Higgins, S.; Stathopoulos, T. Application of artificial intelligence to urban wind energy. *Build Environ.* **2021**, *197*, 107848. [CrossRef]
17. Ellabban, O.; Abu-Rub, H.; Blaabjerg, F. Renewable energy resources: Current status, future prospects and their enabling technology. *Renew. Sust. Energ. Rev* **2014**, *39*, 748–764. [CrossRef]
18. Cho, K.P.; Jeong, S.H.; Sari, D.P. Harvesting wind energy from aerodynamic design for building integrated wind turbines. *Int. J. Technol.* **2011**, *3*, 189–198.
19. Daemei, A.B.; Khotbehsara, E.M.; Nobarani, E.M.; Bahrami, P. Study on wind aerodynamic and flow characteristics of triangularshaped tall buildings and CFD simulation in order to assess drag coefficient. *Ain Shams Eng. J.* **2019**, *10*, 541–548. [CrossRef]
20. Nishi, A.; Miyagi, H.; Higuchi, K. A Computer-Controlled Wind Tunnel. *J. Wind. Eng. Ind. Aerodyn.* **1993**, *46*, 837–846. [CrossRef]
21. Li, J.C.; Hu, S.Y.; Li, Q.S. Comparative study of full-scale and model-scale wind pressure measurements on a gable roof low-rise building. *J. Wind. Eng. Ind. Aerodyn.* **2021**, *208*, 104448. [CrossRef]
22. Sheng, R.; Perret, L.; Calmet, I.; Demouge, F.; Guilhot, J. Wind tunnel study of wind effects on a high-rise building at a scale of 1:300. *J. Wind. Eng. Ind. Aerodyn.* **2018**, *174*, 391–403. [CrossRef]
23. CKP Wind Solutions: Wind Tunnel Model. Available online: http://www.ckpwind.com/ (accessed on 16 February 2014).
24. You, J.; Lee, C. Experimental Study on the Effects of Aspect Ratio on the Wind Pressure Coefficient of Piloti Buildings. *Sustainability* **2021**, *13*, 5206. [CrossRef]
25. Architectural Institute of Korea (AIK). *Korean Building Code-Structural*; Architectural Institute of Korea: Seoul, Korea, 2009; pp. 99–101.
26. Sari, D.P.; Cho, K.P. CFD and wind tunnel analysis for mounted-wind turbine in a tall building for power generation. *Mechatron. Electr. Power Veh. Technol.* **2014**, *5*, 45–50. [CrossRef]
27. Turbulent Flow Instrumentation: Getting Started Series 100 Cobra Probe. Available online: www.turbulentflow.com.au (accessed on 2 January 2018).
28. Sari, D.P. Strategy for Improving Wind Resources from Building Aerodynamic Design for Building Integrated Wind Turbines. Master's Thesis, Wonkwang University, Iksan, Korea, 4 April 2012.
29. Sari, D.P.; Kusumaningrum, W.B. A Technical Review of Building Integrated Wind Turbine System and a Sample Simulation Model in Central Java, Indonesia. *Energy Procedia* **2014**, *47*, 29–36. [CrossRef]